Heat Flow and Thermal History of the Moon

Ye. A. Lyubimova
O. Yu. Schmidt Institute of Earth Physics
Academy of Sciences,
Moscow, U.S.S.R.

An analysis is made of current heat flow data and thermal models of lunar evolution which satisfy the diverse information that has accumulated on internal processes.

Direct measurements of the heat flux were made in drill holes at the Hadley Rille (Apollo 15) and Taurus-Littrow (Apollo 17) regions located on the margins of Mare Serenitatis and Mare Imbrium, which apparently have mascons. These measurements resulted in comparatively high values of the heat flux,

3.1×10^{-6} W/cm^2 $\left(0.74 \times 10^{-6} \frac{\text{cal}}{\text{cm}^2\text{sec}}\right)$

(Apollo 15) and

2.8×10^{-6} W/cm^2 $\left(0.67 \times 10^{-6} \frac{\text{cal}}{\text{cm}^2\text{sec}}\right)$

(Apollo 17), which differ from the wide spread earlier concept of a much lower heat flow from a Moon of chondrite composition. Only a small number of earlier works predicted a high heat flow. Those were the data on the thermal emission of the Moon in the microwave region (ref. 1) and the results of certain calculations of the thermal history of the Moon (ref. 2). Current interpretation of the high heat flow requires a high average concentration of uranium for the Moon—60 ppb—as well as an initial surface temperature sufficient to melt the upper several hundred kilometers, including the lunar crust and lithosphere.

The crust of the Moon is a discrete layer several-dozen-kilometers thick, bears traces of magmatic fractionation that occurred during the period of intensive melting of the uppermost layers of the Moon (hundreds of kilometers deep), and has been reworked by the impacts of meteorites.

Among the sources of initial melting are the following: accretional heating during accumulation of the Moon, possible electrical heating by an early strong solar wind, tidal friction when the Moon was close to the Earth, and the effect of short-lived isotopes. All the sources are problematical. The thermal effect due to collisions of protomoons during accretion appears to be adequate to melt the rocks in the area of impact, but not at great depth (refs. 3 and 4).

At this stage of investigation of the thermal state of the Moon, the following problems are the most significant.

What was the cause of the rapid early melting and differentiation?

To what extent can heat fluxes obtained close to the margin of a mascon be represented as global values? To what extent can an average, presently uniform concentration of uranium be responsible for the surface heat flux that undoubtedly results from irregular distributions of uranium and thorium with depth, due to the rapid fractionation during the accretionary stage? To what extent can coarse numerical modeling of the thermal history of the Moon, where the first step in the calculation grid is 20 km in size (refs. 5 and 6) or where even the smallest is 5 km (ref. 7), reflect the fine structure of the uniquely low thermal conductivity of the upper few meters?

Before the Luna and Apollo flights to the Moon, a lunar model of chondrite composition

was widely used (refs. 2 and 8 through 13). A drastic reexamination of these models was required after study of the chronology of the lunar samples and determination that the lunar K/U ratio was 2000 instead of 80 000 as for chondrites and 10 000 as for the Earth. The low lunar K/U ratios are in agreement with the overall depletion of the Moon in volatile elements.

A comparative study of the energy balance of the Earth and the Moon by Lyubimova (ref. 2) showed that the integral heat loss $Q_{\mathbb{C}}$ for the lifetime of the Moon, the integral heat generation $H_{\mathbb{C}}$, and the total heat content at the melting point of the planet $\Lambda_{\mathbb{C}}$ are in the relationship $\Lambda_{\mathbb{C}} < H_{\mathbb{C}} \approx Q_{\mathbb{C}}$ for the Moon. This means that the energy losses from the surface of the Moon predominate (in distinction from the Earth) over internal heat generation and heat content for the state of complete melting, i.e., the Moon is cooling down. The heat flux at the surface is assumed to be close to the upper limit established by lunar surface radio emission methods (refs. 14 and 15). According to thermal history calculations, the integral heat flux of the Moon should amount to $Q = 1.9 \times 10^{36}$ ergs, while the heat content of a completely molten Moon is $\Lambda_{\mathbb{C}} = 1.6 \times 10^{36}$ ergs (ref. 2). It was concluded that even in the case of a quite low concentration of radioactive elements, in agreement with the chondritic model, the energy is completely sufficient to convert the lunar interior to the molten state.

Direct measurements of the heat flux during Apollo 15 and Apollo 17 permit one to return to discussion of the energetic state of the Moon. They also make it possible, together with radioastronomers, to refine models of the structure of the uppermost layers of the Moon (refs. 16 and 17). Serious limitations on the thermal history of the Moon were introduced as a result of a seismic experiment on the Moon (ref. 18). They indicate the necessity for a high temperature of the lunar interior and the existence of an asthenosphere below 1000 km. On the other hand, the internal temperature derived from the electrical conductivity profile indicates that the temperature of the lunar interior should be less than the solidus temperature (ref. 19). The existence of mascons also requires this because the thickness of the lithosphere must be sufficient to sustain a load corresponding to the mascons. Correspondingly, the viscosity of the lunar interior is assumed to be very high, up to 10^{26} poise (ref. 20). The chronology of lunar volcanic activity shows that all episodes of volcanic activity and excavation of the mare must have ended 3 b.y. ago (refs. 21 and 22). The magnetic history of the Moon indicates that there was an old magnetic field which is responsible for the remanent magnetism of the Moon (ref. 23). This again entails the conclusion that there was intense melting in the initial stages of evolution of the Moon. In this manner, the factual materials returned by the Luna and Apollo missions indicate that the Moon evolved quickly.

In this article, we examine the parameters of lunar thermal models, calculation techniques that consider melting and effective convection, and the expected regional corrections to the heat flux.

Evolution of a Homogeneous Moon

In a number of the most recent works, the heat flux from the lunar interior is compared with an average uniform concentration of uranium (refs. 5, 6, and 23) in a homogeneous Moon.

A strict analytical solution for a body of spherical shape (the Moon in particular) with uniform distribution of heat sources, thermal diffusivity k, density ρ, and heat capacity C, was given by Lyubimova (refs. 2, 24, and 25), in the form:

$$T_{\mathbb{C}}(r,t) = \frac{1}{C\rho}\int_0^t H(\tau)\, d\tau - \frac{RC}{C\rho r}\int_0^t H(t) \times \left[erfc\left(\frac{R-r}{\sqrt{4k(t-\tau)}}\right) - erfc\left(\frac{R+r}{\sqrt{4k(t-\tau)}}\right)\right] d\tau \quad (1)$$

where $R_\mathbb{C}$ is the radius of the Moon and r is the variable radius

$$erfc\ x = 1 - erfx;\ erfx = \frac{1}{\sqrt{\pi}} \int_0^x e^{-\alpha^2} d\alpha$$

The bracket in (1) is the first term of the series of the determinate Green's function (1.6) (see Appendix I):

$$G\ (t,r,t',r') = \sum_{n=0}^{\infty} \left\{ erfc \left[\frac{(2n+1)\ R - r}{\sqrt{4k\ (t-\tau)}} \right] - erfc \left[\frac{(2n+1)\ R + r)}{\sqrt{4k\ (t-\tau)}} \right] \right\}$$

The first term in the expression for temperature gives the temperature of the central region and the second gives the region of heat outflow to the surface. The region of outflow begins at depth:

$$D = R - r \leq 3 \cdot \sqrt{4kt} \qquad (2)$$

If there is no convection, the region of outflow, D, for Earth, Mars, and Venus does not reach the center, while D for the Moon reaches the center.

Analysis of uniform source models of the Moon, with a variable initial temperature $T_0\ (r)$, is useful in searching for the required models of lunar accretion that would provide a high early temperature of the upper layers of the Moon. This analysis should give the required age of the mare basalts and should provide rapid melting and rapid differentiation of the upper few hundred kilometers and a relatively cold lithosphere at the present time. The mineralogy of the lunar rocks indicates a phase of high temperature and low pressure as suggested by Ringwood (ref. 26) in a semiqualitative conclusion (even before the Apollo missions) that the initial temperature curve had maximum values in the upper 200 to 300 km and a gradual drop toward the center (figs. 1, 2). This curve was used in the calculation of Kaula (ref. 29) during interpretation of the lunar gravitational field. Ringwood (ref. 30) intuitively predicted a curve that is close to the curve for $T_0(r)$ given by Hanks and Anderson (ref. 31).

Homogeneous models of the Moon, with such nonuniform initial curves with maxima,

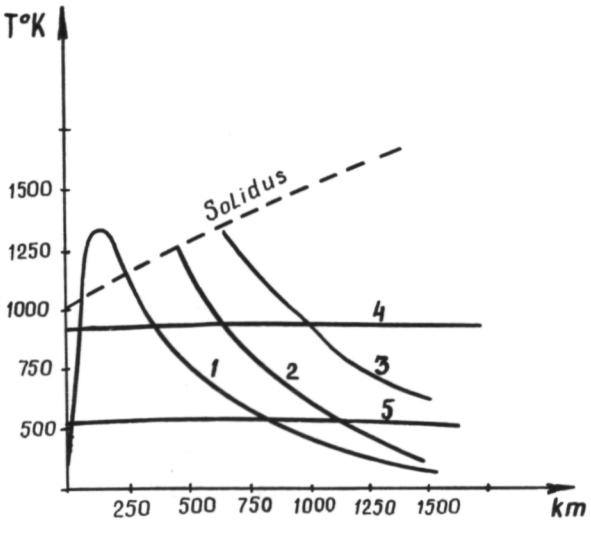

Figure 1.—*Variants of initial temperature distributions in the primitive moon: 1—from Ringwood (ref. 30), 2—from Mizutani (ref. 27), 3—from Hanks and Anderson (ref. 31), 4—MacDonald (ref. 9), Ruskol (ref. 3) (estimated as the result of collision of protomoons), 5—Urey and MacDonald (ref. 28).*

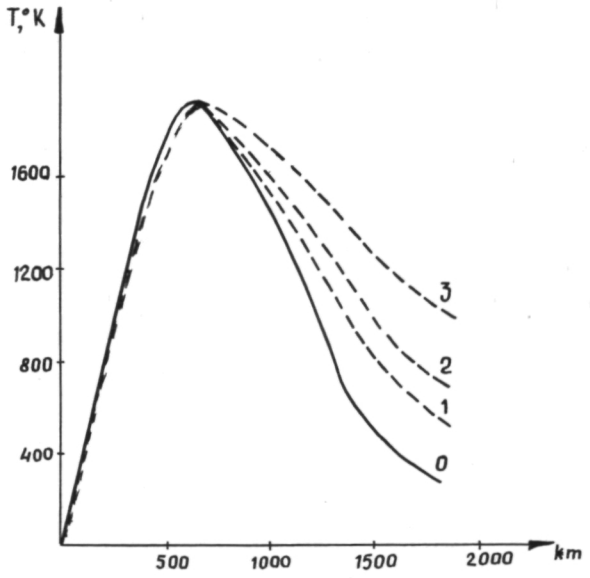

Figure 2.—*Effect of Resorption of Initial Heat with Passage of Time in the Lunar Interior in Absence of Convection (curve 1, fig. 1 is taken as T_0).*

indicate a possible thermal evolution that is dependent on the influence of initial processes. In particular, they permit understanding of the slowness of the disappearance of the maximum $T_0(r)$ and the slowness of propagation of the initial heat inward to the planet. The latter conclusion follows from examination of equation (2), which gives the rate of penetration of temperature by means of heat conductivity in the absence of convection. Initially, the interior of the Moon apparently was cold. The task consists of ascertaining the manner in which the temperature of the central regions of the Moon below 1000 km could reach at the present moment high values sufficient for formation of the aseismic "asthenosphere," the level at which deep moonquakes stop, according to data from low-frequency seismometers (ref. 18).

Evolution of A Heterogeneous Moon

Having selected a uranium content corresponding to the observed heat flux, U = 0.05 ppm in the lithosphere and 0.5 ppm in the crust, we obtain the following models of the lunar thermal history (fig. 3). The temperature curves are compared with the solidus curve of mare basalts, as determined by Ringwood and Essene (ref. 26), in the zone from 100 to 700 km, assuming no convection. The lithosphere thickens for 1.2 b.y. at a rate of 160 km/b.y. Melting proceeds from shallow depths to great depths during the filling of the mare (3.4–3.1)–(3.8–3.6 AE), in agreement with the depth of origin for mare basalts, according to petrogenetical theory (ref. 32). Moreover, a sufficiently thick lithosphere is provided as required to support the stresses connected with the mascon gravitational anomalies. Between 1 and 2 AE there occurred conditions for the existance of a convecting core of undifferentiated lunar material which contained approximately the original concentrations of radioactive elements. The core grew to a radius of 1200 km at 3 AE, then slowly decreased because the concentration of heat sources decreased with time. The chronology, mineralogy, and petrography of the lunar mare basalts indicate a definite sequence of events in differentiation and fractionation of the material. For example, the mare basalts evidently had to be formed during the second thermal cycle, if there was one, i.e., 3.4 to 3.7 b.y. ago, at depths on the order of 200 to 300 km as a result only of endogenous factors. Crater formation apparently mainly ended during the first, most intensive, phase of differentiation and fractional crystallization.

The heterogeneity of the internal structure of the current Moon is demonstrated by the low-frequency seismic experiment, data on the electrical conductivity distribution in the Moon, the existence of an ancient magnetic field, and gravitational data. A schematic section of the heterogeneous Moon was given by Anderson (ref. 33). The Moon consists of a crust, lithosphere, asthenosphere, and, possibly, a core. The upper layer of the crust is composed of mare basalts. The lower layer of the crust is composed of gabbroic anorthosites; under them is a layer of refractory crystals, and even plagioclase or pyroxenes, at depths of 60 to 80 km (ref. 34). The requirement for the absence of large-scale melting in the upper 1000 km imposes significant limitations on the thermal evolution of the Moon (ref. 6).

The chronology of volcanic activity and the concentration of radioactive elements toward the surface are evidence of intensive differentiation at an early stage of lunar development (ref. 35). There are two points of view on the differentiation process. Differentiation may be the result of a relatively rapid accretion and subsequent general melting or of initial chemical stratification during the accretion process.

If the measured values of the heat flux 0.74–0.67 $\times$ 10^{-6} cal/cm^{2}sec (ref. 36) represent the average heat loss characteristic of the entire Moon, the average uranium concentration in the lunar lithosphere must be in the 50- to 80-ppb range.

Attenuation of seismic waves depends strongly on temperature, showing a rapid

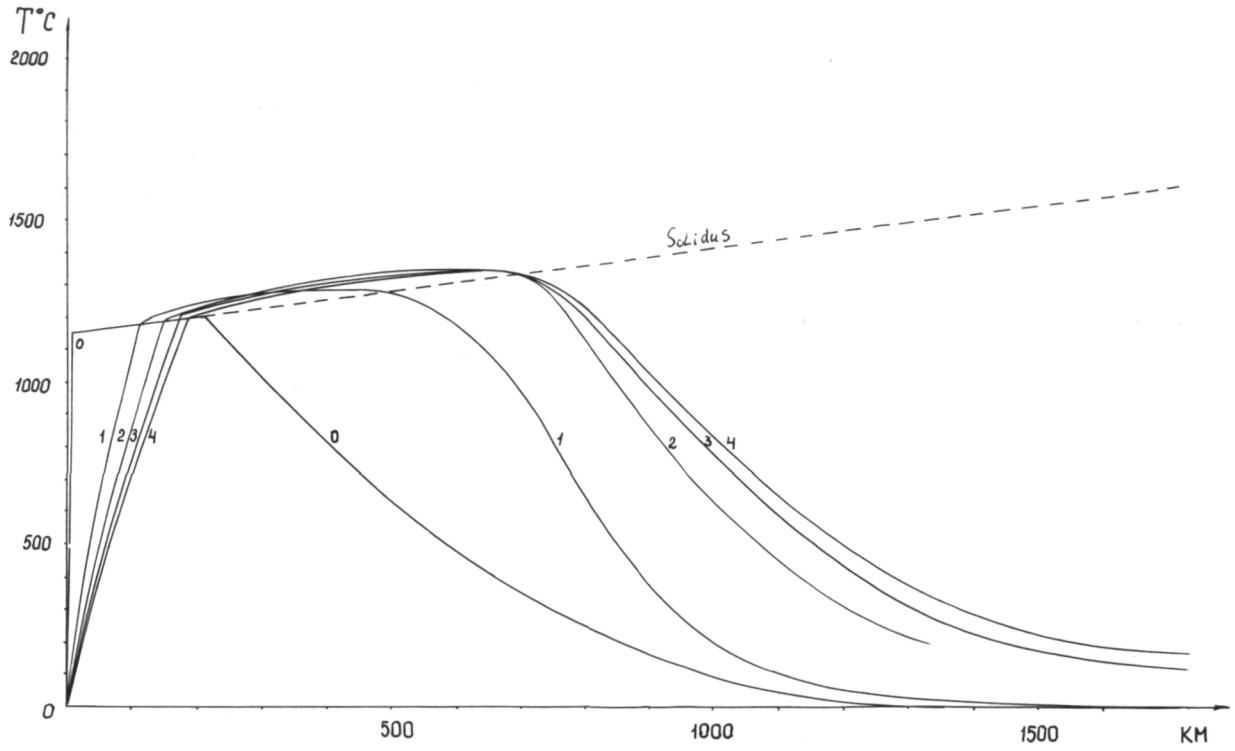

Figure 3.—*Thermal evolution model for a heterogeneous Moon (this work) K/U-2000, Th/U = 4, U = 0.5 ppm in crust and U = 0.05 ppm in lithosphere. Initial temperature taken from Ringwood (ref. 30).*

increase with temperature and a sharp increase with the onset of melting (refs. 23 and 37). Partial melting, with several percent of melt, can explain existing seismic data (ref. 23). The foci of moonquakes for which the depths were determined (18 cases) are concentrated in the 800- to 1000-km range; i.e., there is a concentration of lunar seismic activity in a zone 200 km thick.

The silicate interior of the Moon has a solidus temperature from 1620 K to 1950 K at depths from 100 km to the center. This is compared with some thermal models (ref. 23).

Geological and geochemical processes on the Moon are considerably more primitive than the processes of crustal formation on the Earth. Magmatic activity on the Moon leads to eruption of magma and formation of gabbro-basalt-type rocks similar to the magmatic rocks of the Earth. Differences are connected with the enrichment of the Moon with lithophile, refractory element, and the loss of a part of the siderophile elements. The depths of formation of magma chambers on the Moon, the rate of rise of magma, the temperature, and the diversity of surface crystallization conditions are reflected in the structure and texture of the rock (ref. 38). High concentrations of FeO, TiO_2, and other elements reduce the crystallization temperature of the magma. The ratios of close isomorphic pairs of chemical elements K/Rb, Ca/Sr, Th/U approach the same ratios as in the tholeiite basalts of the Earth (refs. 22 and 39).

One of the hypotheses of the origin and evolution of the heterogeneity of the Moon which deserves attention is the hypothesis of convection (ref. 40). The following expression for liquid flow of a cellular structure is obtained between the Nusselt (Nu) and Rayleigh (Ra) criteria which describe convective heat transfer:

$$Nu = 0.205\ Ra^{1/4}$$

$$Nu = \frac{\alpha l}{\lambda};\ Ra = \frac{g\beta}{\nu a} A l^4; \qquad (3)$$

α is the heat transfer coefficient, l is the thickness of the liquid layer, λ is the thermal conductivity coefficient, a is the thermal diffusivity coefficient, ν is the kinematic viscosity coefficient, β is the bulk expansion coefficient, g is the acceleration of gravity, and A is the temperature gradient in the layer.

Experiments with various liquids at $4000 < Ra < 10^5$ have shown that equation (3) describes the test data well. The value of Ra_{crit} (which determines the start of the convective process) proved to be 3100 according to the experimental data. Thus, the convective process starts at the moment when $l \geq l_{crit}$, where

$$l_{crit} = \sqrt[4]{\frac{3100\ \nu a}{g\ \beta\ A}} \qquad (4)$$

Let the wall temperature be T_1 and T_2 and $(T_1 \leq T_2)$. The magnitude of the heat flux from the hotter wall will be

$$Q = \alpha\ (T_1 - T_2) \qquad (5)$$

On the other hand,

$$Q = \lambda_{ef} \times A \qquad (6)$$

The quantity A can be assumed to be equal to the melting temperature gradient, since it is known from geochemistry that moving melts are not superheated. Besides, this follows also from physical considerations, since the values of T_1 and T_2 are essentially the melting temperatures of rocks.

Thus, we write relationship (3) in the form

$$Q = lA\alpha \qquad (7)$$

Then, from relationships (3, 6, and 7) we obtain

$$\lambda_{ef}/\lambda = 0.205\ Ra^{1/4} \qquad (8)$$

The values of λ_{ef}/λ were calculated for a melt under Earth, Mars, and Moon conditions.

Parameters adopted in the CGS system are shown in Table 1.

Table 1.—*Parameters for Calculation by Equation (8)*

		a = 0.01; $A = 3\times10^{-5}$		
	g, 10^3	β, 10^{-5}	l_{crit}, (km) $\nu = 10^{19}$	$\nu = 10^{20}$
Earth	1	2.0	47	84
Moon	0.16	4.0	64	113
Mars	0.39	3.5	52	93

Parameters of Thermal Models

The basic parameters of thermal models are the coefficients of heat transfer, heat capacity, latent heat of phase transitions, and the heat sources. The coefficient of heat transfer includes the coefficient of molecular (phonon) heat conductivity of a solid $\lambda\phi$, radiant heat transfer λ_r, as well as the effective heat transfer by convection λ_{ef}. A family of $\lambda\phi$ and $\lambda\phi + \lambda_r$ curves for the presumed rocks of the Moon are presented in figure 4. At high temperatures, the coefficients change between the bounds of 0.003 and 0.012 cal/cm · s · K, and it is very likely that, deep in the interior of the lunar lithosphere, the value of the thermal conductivity is close to constant, at 0.07 cal/cm · s · K = 2.8 W · m^{-1} · K^{-1}.

The unique thermal properties of the low-conduction surface layer of the Moon must play a significant role in the heat balance

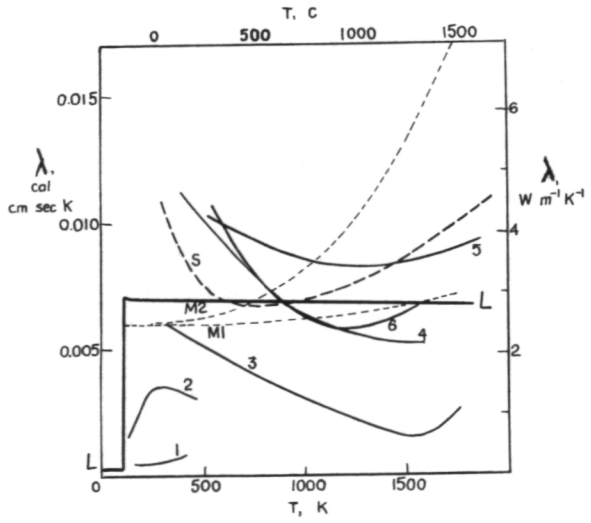

Figure 4.—*Thermal conductivity coefficients for lunar rock (curves 1–6 correspond to Toksöz and Solomon (ref. 23); curve L, this work).*

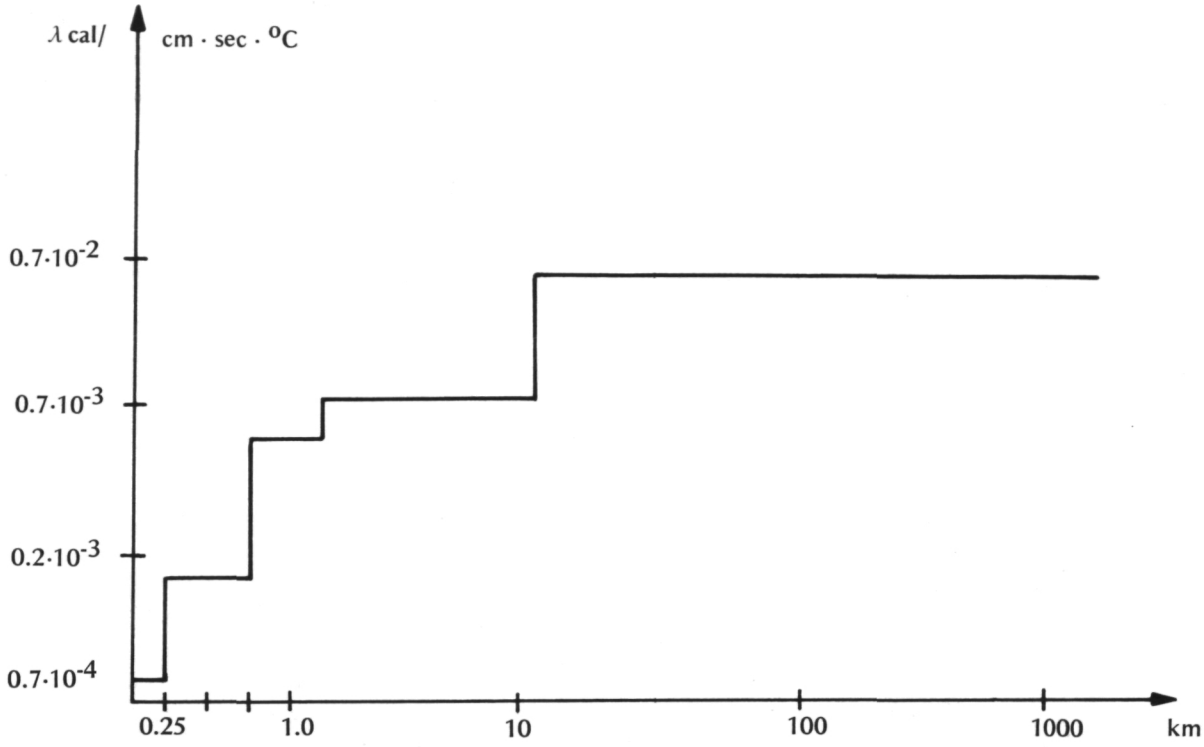

Figure 5.—*Model of step wise change in thermal conductivity used in calculations of evolution of heterogeneous Moon.*

and evolution of the heat flux. In connection with this, we have studied in greater detail than has been done previously the thermal conditions of contemporary models of the Moon, with the sharp change in thermal conductivity taken into account by means of the maximum possible decrease in the interval of temperature calculations close to the surface. Our initial model of thermal conductivity distribution is given in figure 5 and table 2:

The thermal isolation layer at the surface of the Moon is of significant value for prolonged retention of the melt in the interior of the Moon. If λ = const = 0.007 cal/cm · s · deg., it persists for 300 m.y.; if λ is according to table 2, it persists for 1.3 AE.

Table 2.–*Initial Model of Thermal Conductivity Distribution*

Depth, km	Thermal Conductivity λ, cal/cm • s • deg.
0–0.250	7×10^{-5}
0.250–0.750	7×10^{-4}
0.750–1.000	7×10^{-3}
1km–10km	7×10^{-2}
10km–1000km	7×10^{-2}
1000km–1740km	7×10^{-1}

The model of heat generation in the interior of the Moon is determined by the content of uranium, thorium, and potassium. The Luna and Apollo missions demonstrated that the chondrite model of the Moon is not correct (ref. 22). Several variants of U, Th, and K content were tried in numerical calculations.

For the case of uniform distribution of heat sources, variants with the maximum B and minimum A in content were taken:

A: U = 0.5 ppm
B: U = 0.8 ppm

After formation of a crust with layers 20 and 60 km thick and a lithosphere (1000 km), redistribution of sources leads to approximately a twentyfold depletion of uranium, according to the model of Vinogradov (ref.

22). According to these data, the concentrations of the elements in the upper 20 km was:

$U = 2.3 \times 10^{-7}$ g/g; Th $= 0.9 \times 10^{-7}$ g/g; K $= 0.83 \times 10^{-3}$%.

After stratification, the following remained in the lithosphere:

$U = 0.43 \times 10^{-8}$ g/g; Th $= 0.38 \times 10^{-7}$ g/g; K $= 0.83 \times 10^{-3}$%.

During melting, the physical parameters of the phase transition boundaries are disrupted. This disturbs the stability of the calculation schemes, if special smoothing procedures are not used. The effects of melting and convection on temperature were modeled using a technique described by Budak et al. A smoothing function of the physical parameters at the phase transition boundary was introduced. When the temperature T^M (r,t) becomes higher than the melting temperature, the thermal conductivity coefficient is replaced by an effective heat transfer coefficient $\lambda_{ef} = 0.1$–0.05 cal/cm · s · ° C, symbolizing convection.

The heat sources are the most important in calculations of the thermal history. The abundance of isotopes measured in lunar samples and by means of orbital gamma-ray observations (ref. 41) leads to the conclusion that the concentrations of uranium and thorium in the surface layers of the Moon are increased over those in the deep layers and are generally higher than on Earth. At the same time, the Moon is depleted in volatiles, including potassium. While for Earth K/U = 10 000 and for chondrites K/U = 80 000, we have only K/U = 2000 for the Moon. Using the ratio K/U = 2000, we obtain the average generation of heat $H(r,t)$ in the interior of the Moon as a simple function of the bulk uranium content $U(t_0)$:

$$H(r,t) = \rho\, U(\tau_0)\, 1.35\, [0.73 + 0.20\, \mathrm{Th/U} + + 0.25 \times 10^{-4}\, \mathrm{K/U}]$$

$\rho = 3.34$ g/cm³

$U_0 = 7.3 \cdot 10^{-6}$ g/g $= 7.3$ ppm

After stratification during the first billion years, the crust of the Moon consists of 20 km of basalts and 40 km of andesites; the Moon is considered to be three-layered, according to Anderson (ref. 33).

The average content of uranium is between those of howardites and eucrites and determines the average value of the global heat flux which is 33 erg/cm² · s (ref. 42). The decay constants, decay energy, and isotope abundances are taken in accordance with reference 43. We disregard the value of tidal friction, including it in $T_0(r)$.

Direct and Indirect Determination of Heat Flux and Structure of the Lunar Crust

Before the flights to the Moon of the Luna and Apollo 15, 16, and 17 spacecraft, the heat flux on the Moon was determined by study of its natural radio emission and extraction of the constant components that determine the temperature gradient in the interior. Precision measurements of the constant component of the radio temperature, at two wavelengths, μ_1 and μ_2, perpendicular to the surface, give an expression for the temperature gradient (refs. 15 and 44).

$$\mathrm{grad}\, T(z) = \frac{dT_{e0}}{d\mu} \frac{1}{(1 - R_\perp)\, m l_t}$$

where T is the average effective temperature over the disk, depending on μ; $R_\perp$ is the albedo; and l_e/l_t is the ratio of the depth of penetration of electromagnetic and thermal waves, $\delta_1/\mu = m$.

The quantity l_e, the depth of penetration of electromagnetic waves, is proportional to wavelength μ and inversely proportional to tan Δ, the tangent of the loss angle (ref. 44):

$$l_e = \mu/(2\pi \sqrt{\varepsilon}\, tan\Delta) = \tilde{a}\, \mu$$

where ε is the dielectric constant and $\tilde{a}$ is a proportionality coefficient, depending on the properties of the substance in which

$$\tan \Delta = 2\sigma/\varepsilon f$$

Here, σ is the effective electrical conductivity at a given frequency f. Multiplying grad T by the thermal conductivity coefficient λ, we obtain the heat flux,

$$q_{\mathbb{C}} = \frac{dT_{e0}}{d\mu} \frac{\sqrt{\pi}}{(1 - R_\perp)\, m\gamma \sqrt{t}}$$

Using the model of heterogeneous lunar surface structure (rocks with ρ_1 covered by a porous layer with ρ_2), Tikhonova and

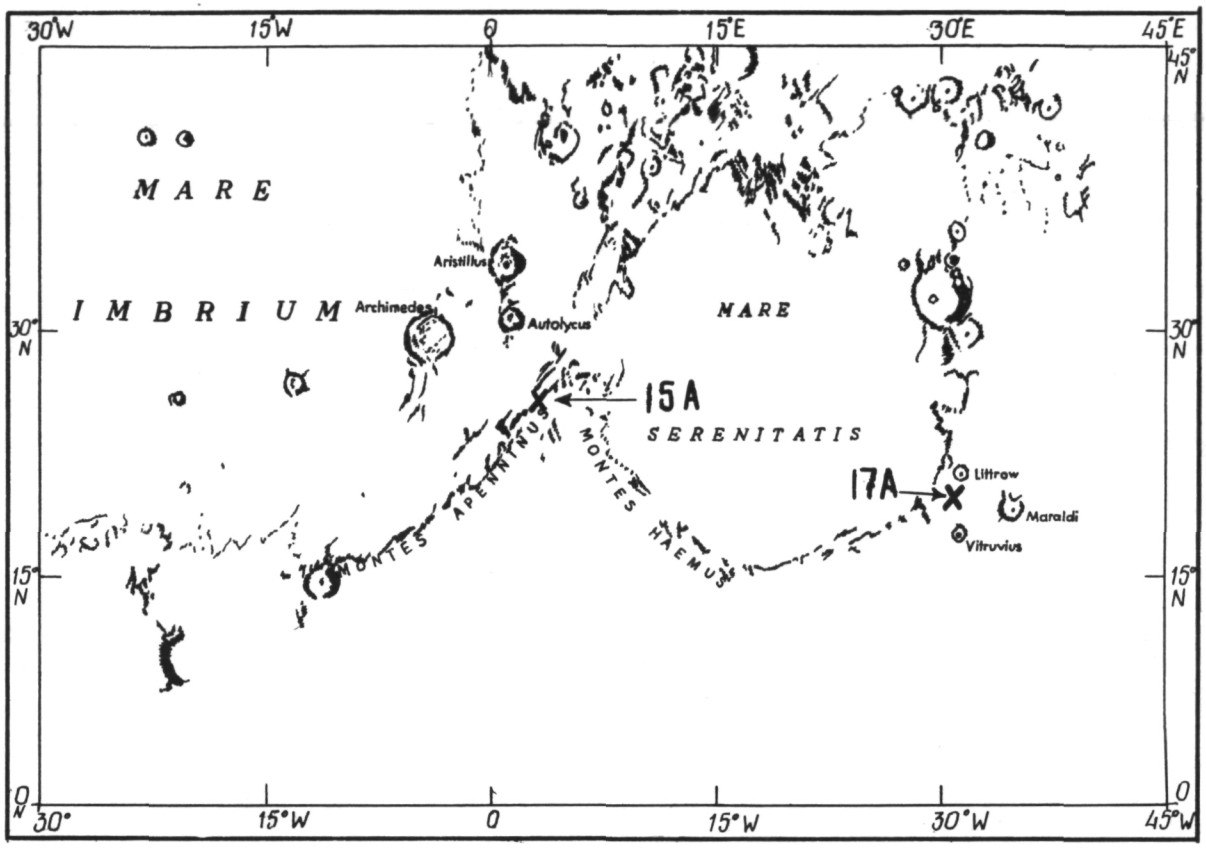

Figure 6.—*Location of heat-flux measurements by the Apollo 15 and Apollo 17 programs.*

Troitskiy (ref. 15) predicted the relatively high value of the heat flux from the interior of the Moon: $0.7 \times 10^{-6} < q_{\mathbb{C}} \leq 0.95 \times 10^{-6}$ cal/cm^2 • s.

Direct measurements of the heat flux in boreholes provide significant information on the heat balance and evolution of the Moon. Direct measurements of the heat flux from the interior of the Moon, with and without introduction of regional corrections (Apollos 15 and 17), showed that the value of the heat flux is at the upper limit of the expected values given on the basis of geochemical models, the intensity of radio emission, and calculations of the thermal history of the Moon. The two groups of measurements indicated were made at the margins of Mare Serenitatis and Mare Imbrium, at the boundary of the assumed mascon basins (fig. 6). The thick lunar crust contains significant irregularities. Particularly large irregularities are concentrated on the visible side of the Moon.

Similar boundaries are connected with change in the physical-chemical properties. In this connection, it is natural to expect a change in the thermophysical properties in the transition from the mare regions to the highlands. In fact, investigations by Luna 21 (Lunkhod 2) in the region of the eastern margin of Mare Serenitatis (as well as Lunokhod 1 in Mare Imbrium) showed that, according to the data of the RIFMA–M instrument, the iron content in the highlands is less than in the mare. According to radar observations, the region of measurement of the thermal flux was close to a "black spot region." The blue tint of these spots also is evidence of a high concentration of iron and titanium ions, with which variations in the coefficient of thermal conductivity and refraction of the heat flux may be connected. Terrestrial ex-

perience with heat flux measurements indicates the unreliability of judgments as to the average heat loss, q, on the basis of one or two measurements.

On the other hand, the absence of even a small region of water and appreciable tectonic activity permits one to assume that local variations in the heat flux on the Moon will be less than on Earth. However, the specific factors of disintegration and erosion of the surface of lunar rock (meteorite impacts, thermoelastic stresses as a result of fluctuations of the surface temperature, the effect of the mascons as inclusions of extraneous thermal conductivity) could be reflected in the history of the heat flux. The phenomena of disintegration of the lunar surface rocks by meteorite impacts should have introduced local changes in the energy balance of the surface.

The places of measurement of the heat flux in the boreholes on the Moon are presented in figure 6. They are located at the edges of Mare Serenitatis and Mare Imbrium. The Apollo 15 borehole is in the region of the Appennine Mountains, between Mare Serenitatis and Mare Imbrium and distant from three craters, Autolycus, Aristillus, and Archimedes. The landing site of Apollo 17 is located in the Taurus-Littrow Valley. There is a cross section of the latter, according to seismic sounding data, given in figure 7 (ref. 45). We made an attempt to determine the shape of the heat flux anomaly at the edges of the mascon, on the basis of numerical modeling of a two-dimensional structure, containing inclusions with high or low thermal conductivity as functions of varying degrees of burial (fig. 8). Data on thermal conductivity of the lunar rock and observed variations in them were used. Two mascon models were used (figs. 8 and 9), with and without allowance for the relief. In accordance with conclusions from the data of Luna 10, it was assumed that the surrounding surface rock of the Moon was basaltic.

The heat-flux anomaly has the appearance of sign-changing curves on the boundaries of trough-shaped (fig. 9) and rectangular (fig. 8) irregularities. With movement of an inclusion to the surface, a false anomaly at its edge can exceed 20 percent, with a threefold thermal conductivity drop. The size of the anomaly can increase due to a sudden increase in uranium concentration. On the lunar highlands and mare, Langseth et al. (refs. 16 and 17) used the observed q and more accurately determined the structure of the cover.

The absence of water and of noticeable

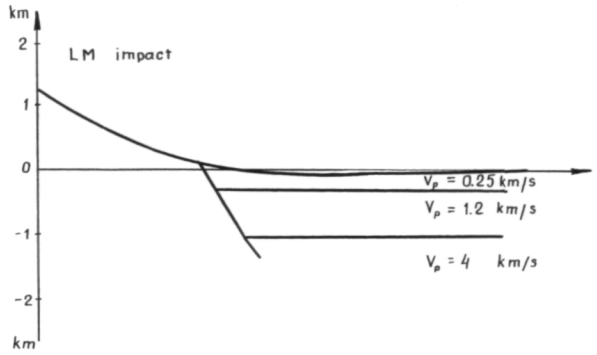

Figure 8.—*Change in relative value of heat flux* q/q_0 *above horizontal conducting inclusion (A) (cross hatched) with thermal conductivity* λ_2 *three times the thermal conductivity* λ_1 *of the surrounding rock, and above a thermal insulating inclusion (B). Curves 1, 2, and 3 correspond to depths of burial: (1)* H = 0, *(2)* H = 1 km,, *(3)* H = 2 km.

Figure 7.—*Cross section of the structure of the lunar crust in Apollo 17 landing region, from seismic data; line A–B, assumed fracture (ref. 45).*

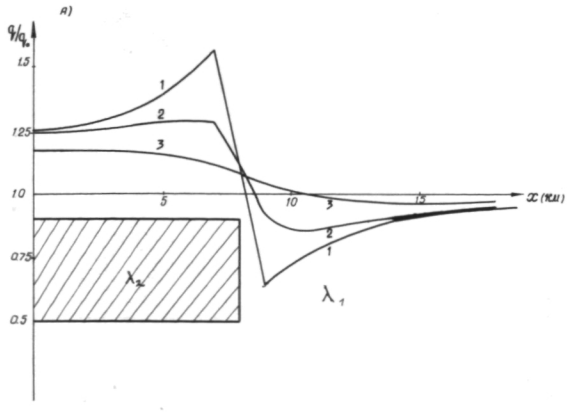

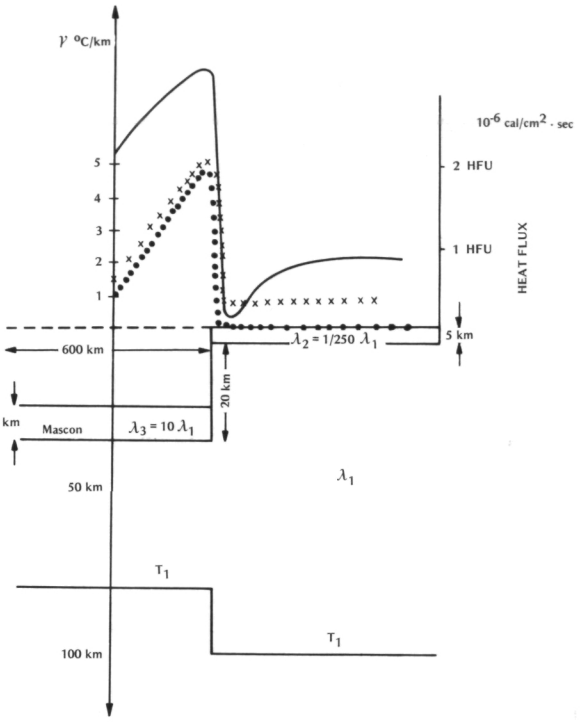

Figure 9.—*The thermal effect of a conducting mascon ($\lambda_3 = 10\ \lambda_1$), buried 20 km in a poorly conducting layer ($\lambda_2 = \lambda_1/250$) and with a high temperature T_1 at the level of the compensating layer.*

tectonic activity on the surface of the Moon allows one to assume that local variations in the heat flux on the Moon will be less than on Earth. However, disintegration and erosion of the surface layers by meteoritic impacts has severely disrupted the surface layer. Whether or not the direct measurements of the heat flux (refs. 16 and 17) by Apollo 15, 16, and 17 are representative involves data on the structure of the upper layer.

Research of Troitskiy et al., (ref. 44), Tikhonova and Troitskiy (ref. 15), and Langseth and Keihm (refs. 16 and 17) was devoted to study of the nature of the material and its density and heat conductivity. Significant change in the heat conductivity of the regolith and deep underlying layers was demonstrated in these researches by independent methods. In the work of Langseth and Keihm (ref. 36), the condition of a 15-cm layer of the regolith is studied in detail. At the same time, in work on the thermal history of the Moon, one studies the distribution of the thermal parameters on a considerably rougher scale which is unsatisfactory for calculation of the heat flux.

Calculation Procedure

The analytical solution for temperature and heat flux presented in Appendix I is a general solution that is universal for spherical planets of any radius, for stages when the distribution of heat sources and thermophysical parameters can be assumed to be uniform but, permitting change with time (e.g., a decrease in the concentration of radioactive elements because of their continuous decay).

In all later stages of development of planetary bodies, with the exception perhaps of the asteroids, the distribution of properties and of heat sources in particular is irregular, and differentiation, melting, and convection are included. The problem is solved with computers, using the method of finite differences. Any temperature distribution given by a computer is a partial solution. In principle, there can be an infinite number of such solutions from the point of view of thermal conductivity theory. In our numerical examples, the thermal conductivity equation was approximated by a finite difference scheme, with steps h along the axis r and along the time axis t (Appendix II). During melting, part of the thermal energy must have been absorbed as the latent heat of fusion.

Thermal conductivity problems, with phase transitions on the moving interface of two phases taken into consideration, are known in thermophysics as the "Stefan problem." Current models of the thermal evolution of the surface molten layer of the Moon (refs. 23 and 13) show that this layer is gradually displaced inward, with melting occurring on the lower boundary, while solidification and crystallization occur on the upper. In this manner, we must consider the Stefan problem for two moving boundaries: the upper $z = x_1\ (t)$ and the lower $z = x_2\ (t)$. It is controlled by the heat balance conditions in the form

$$L\rho\frac{dx_1(t)}{dt} = \lambda_1\frac{\partial T_1}{\partial z}\bigg|_{z=x1} - \lambda_2\frac{\partial T_2}{\partial z}\bigg|_{z=x2}$$

$$L\rho\frac{dx_2(t)}{dt} = -\lambda_2\frac{\partial T_2}{\partial z}\bigg|_{z=x2} + \lambda_3\frac{\partial T_3}{\partial z}\bigg|_{z=x2}$$

where z is the depth; λ_1 and λ_3 are the thermal conductivities above and below the molten layer; λ_2 is the coefficient of heat transfer or effective thermal conductivity inside the molten layer, possibly with inclusion of convective transport; L is the latent heat of fusion; and T_1 is the temperature in the upper solid layer, satisfying the boundary conditions:

$$T_1(z)\big|_{z=0} = 0$$

$$T_1(z)\big|_{z=x1(t)} = T_m\,[x_1\,(t)]$$

$$T_m = T_0 + \gamma_2 z$$

Here, T_m is the melting temperature, and γ_2 is the melting temperature gradient. Let T_2 be the temperature inside the molten layer, satisfying the conditions:

$$T_2(z,t)\big|_{z=x1} = T_m\,[x_1\,(t)]$$

$$T_2(z,t)\big|_{z=x2} = T_m\,[x_2\,(t)]$$

T_3 is the temperature in the lower layer below the level of the melt, satisfying the conditions:

$$T_3(z,t)\big|_{z=x2} = T_m\,[x_2\,(t)]$$

$$\frac{\partial T_3}{\partial z}\bigg|_{z=x2} = \gamma_2$$

The initial conditions for the moving boundary are the following:

$$x_1(t)\big|_{t=0} = a, \qquad x_2\,(t)\big|_{t=0} = b$$

The Stefan problem is nonlinear. The nonlinearity increases if the dependence of thermal conductivity on temperature is taken into consideration. In order to carry out automatic soothing of jumps in the physical parameters on the phase transition boundaries, we use the smoothing method of Budak et al. and we introduce a change of the variables

$$T = U + T^*$$

and the specific heat content function (see Appendix III)

$$H\,(u,r) = \int_0^u [c(\zeta)\rho(\zeta) + .L\rho\delta(\zeta - T^*)]\,d\zeta$$

The difference analog of the thermal conductivity equation is given in Appendix III. The value of the latent heat is assumed to be $L = 400$ J/g. The surface temperature is assumed to be constant during the life of the Moon and equal to $-20°$ C.

The temperature distribution should be satisfied by the data of a comparatively high heat flux (refs. 16 and 17). The value of q, previously calculated from theory for the present and with the age of the Moon being 4.6×10^9 yr, is 0.36×10^{-6} cal/cm^2 • s (ref. 2). A molten layer forms at 2.1×10^9 yr, at a depth of 500 km, with a 150-km width and, at 3.2×10^9 yr, the melting level reaches 300 km and is maintained up to the present time.

The hot state of the Moon could be explained in this manner, but the model does not completely satisfy the heat flux and the heterogeneous seismic structure. Better agreement with the seismic model and geochemical evolution is obtained by assuming higher uranium content up to a value of 60 ppb in a homogeneous Moon, which corresponds to the models of Toksöz et al. (ref. 46) and Toksöz and Solomon (ref. 23). In figure 3, with an initial formation of a melt, the effect of the latent heat on the phase transition boundaries was taken into account: absorption of 400 cal/g at the upper boundary and emission on the lower boundary of the melt, in accordance with Stefan's law for a moving boundary. The latent heat was incorporated in the thermal conductivity equation through the specific heat content by the method of Budak, and the solution of Stefan's problem then has the form of Appendix III. At the onset of melting, the heat transfer increases, and the coefficient λ increases tenfold. If one assumes differentiation at the very start and a crustal thickness of 60 km with uranium concentration 0.4×10^{-6} g/g, then a melt forms in the lithosphere at a depth of 100- to 600-km and quickly expands, and the greatest heat flux reaches 1.17×10^{-6} cal/cm^2 • s (1 AE) and is 0.6×10^{-6} cal/cm^2 • s at present, which is in agreement with the heat flux predicted by Tikhonova and Troitskiy (ref. 15) and measured by Langseth and Keihm (refs. 16, 17, and 36).

Consequences of the Thermal History of the Moon

Study of moonquakes and lunar tectonics by high-frequency seismometers has shown that thousands of very small lunar signals recorded by the Apollo 14, 15, and 16 stations are correlated with meteorite impacts, as well as with the sunrise and sunset periods. This correlation of micromoonquakes with the thermal cycle on the surface indicates that a considerable fraction of the micromoonquakes are of a thermal nature (ref. 47). There are two likely mechanisms of such periodic thermal moonquakes: (a) fracturing of the lunar rock and (b) slippage of lunar soil along slopes, caused by the periodic thermal stresses. The moonquake signals recorded by high-frequency seismometers are completely different from locally generated moonquakes. In conformance with current seismic models of the structure of the Moon, deep moonquakes arise at the base of a thick elastic shell (lithosphere), immediately above the boundary of the relatively weak central zone of the asthenosphere. Surface tectonic characteristics indicate the possibility of a slight tension on the lithosphere of the Moon in the past when the interior of the Moon became warmer. However, the absence of moonquakes at shallow and intermediate depths at present leads to the assumption that no appreciable compression or dilation rates exist now. Therefore, the Moon should be close to thermal equilibrium, and the rate of heat loss by radiation of heat from its surface should be approximately compensated by the rate of internal heat generation.

Seismic and tectonic activity of the Moon is extremely low compared with Earth. The Moon is characterized by an inactive outer layer 1000 km thick. The seismic hypothesis can be tested from the point of view of thermal processes by calculation of the thermoelastic state of the Moon, with allowance for the fact that its upper layer has already passed through a molten state and that the central layers are now in a softened state close to partial melting or the beginning of melting, i.e., the solidus.

The great thickness of the lunar lithosphere, compared with that of Earth, most likely explains the strongly differing tectonics of these planets.

An estimate of the propagation of elastic deformations and stresses that result from heating and cooling of the Moon can be carried out for models of an elastic, spherical layer placed on the surface of a molten layer.

For a maximum estimate of the expansion of the perimeter of the Moon, the elastic model can be used. The change in radius of an elastic Moon during its thermal history can be estimated by the formula

$$\frac{dR_{\leftmoon}}{dt} = \frac{\alpha}{c\rho}\left(- q_{\leftmoon} + \frac{HRa_{\leftmoon}}{3}\right)$$

where q is the heat flux at the surface, α is the coefficient of thermal expansion, and H is the heat generation. In 1960, the rate of expansion of the Moon was estimated by MacDonald, and in 1968 by Lyubimova, on the basis of chondrite models of the Moon and of a comparatively low heat flux taken from calculations of the thermal history. We have available at present independent, directly measured values of $q_{\leftmoon}$ and U. We substitute the following values of the flux $q_{\leftmoon} = 28$ erg/cm^2 · s, according to Langseth et al. (refs. 16 and 17) and heat generation based on the average uranium content U = 60 ppm and the value $\alpha = 3 \times 10^{-5}$ deg^{-1} (ref. 23). By substituting these numerical values, we obtain 10^{-6} cm/yr for the maximum rate of change in radius of the Moon in the last billion years of its evolution. The rate of change in the radius of the Moon was greater in the past than now. Deformation u and tangential stresses and τ on the surface $r = R$, in the presence of a molten layer, can be determined from the equation of elastic equilibrium in a spherical layer bounded on the inside ($r = a$) and outside ($r = R$) by spherical boundaries. The following are conditions on these boundaries: the upper one is free, and a normal stress is assumed on the lower one, designated conventionally by γ. For a given temperature distribution, we obtain deformation

$$(1 - s)\frac{du}{dr} + 2s\frac{u}{r}\Big|_R = 0$$

and also,

$$(1-s)\frac{du}{dr}+2s\frac{u}{r}\Big|_a=\frac{\gamma}{E}(1+s)(1-25)$$

i.e., the increase in radius u (R) and tangential stress $\tau(R)$ on the surface

$$u(R)=\frac{R}{R^3-a^3}\int_a^R d(r)T(r)r^2dr-\frac{\rho gR^2(1-2s)}{5E}\left[1+\frac{3(3-s)}{4(1-2s)}\cdot\frac{a^3(R^2-a^2)}{R^2(R^3-a^3)}\right]+\frac{\delta(a)T(a)(1-s)}{2(1-s)}\frac{a^3R}{(R^3-a^3)}-\frac{3}{2}\frac{\delta}{E}(1-s)\frac{a^3R}{R^3-a^3};$$

$$\tau(R)=-\frac{E}{2(1-s)}\frac{1}{R^3-a^3}\int_a^R\alpha(z)T(r)r^2dr+\frac{\rho gR(1-2s)}{10(1-s)}\left[1+\frac{3(3-s)}{4(1-2s)}\frac{a^3(R^2-a^2)}{R^2(R^3-a^3)}\right]-\frac{E\alpha(a)T(a)}{4(1-2s)}\frac{a^3}{R^3-a^3}+\frac{3}{4}\gamma\frac{a^3}{R^3-a^3}$$

from which we have

$$\tau(R)=-\frac{E}{2(1-s)R}u(R)$$

The formation of fractures on the surface of the Moon is possible only upon reaching τ, the limit of the strength of the material. From the relationship between u and τ just obtained, the magnitude of the fractures can be estimated, if the value of the critical stess τ_{crit} is substituted in the left side. We assume that on the boundary $r=a$ $\sigma_{rr}=\gamma$. Since the radial component of the stress in a liquid is given by the formula

$$s_{rr}=-p+2\nu\rho_l\left[\frac{\partial v_r}{\partial z}-\frac{1}{3}\operatorname{div}\vec{v}\right]$$

$$v_0=v_a=0$$

on the boundary, $r=a$ and $\sigma_{rr}=\gamma$

$$\gamma=p(a)=2\nu\rho_l\left(\frac{\partial v_r}{\partial z}-\frac{1}{3}\operatorname{div}\vec{v}\right)$$

where ρ_l is the density of the melt. The formula for determination of the increase in perimeter of the Moon will have the form:

$$\frac{u(R)}{R}=\frac{1}{R^3}\int_a^R\alpha Tr^2dr+\frac{\alpha(a)T(a)a^3}{3R^3}-\frac{\rho gR(1-2s)}{5E}\left(1-\frac{a^5}{R^5}\right)+\frac{s(1-s)\nu\rho_0(\bar{v}+\bar{v}_\tau)ab}{ER^3}\left[1+\frac{2\alpha_l\theta}{3(1+\alpha_l)\theta}\frac{(\bar{v}+\bar{v}_\tau)b}{\kappa_0}\right]\left[\frac{1}{1-\exp\frac{(\bar{v}+\bar{v}_\tau)(a-b)}{\kappa_0}}\right]$$

Calculations show that the perimeter of the Moon increased during the first half billion years and then began to decrease until the time of formation of the asthenosphere. If the assumption of the existence of the strong convective heat transfer in the region of the partially molten asthenosphere of the Moon is introduced, an increase in the perimeter again resulted 2 to 3 b.y. ago. It is as though the molten layer expands the Moon from inside, and the increase in the perimeter ensures formation of crustal fractures through which the magma erupts.

Conclusions

The principal attention has been given in this work to an effort to relate the values of the observed heat fluxes to the thermal evolution of the Moon, considering the fine structure of the outer crust which has the properties of a uniquely insulating material.

In calculations of the history of the heat flux, extremely small depths (steps in the calculation network of 250 m in all) were introduced into analysis of the numerical determinations of temperature differences (on the order of hundreds of meters), with allowance for abrupt differentiation in the thermophysical properties and for heat generation.

In this work, initial melting of the upper 250 km was assumed, with allowance for abrupt stepwise differentiation of the thermophysical properties and heat generation, as well as for the rapid fractionation of matter. The analysis included the effects of absorption and emission of heat at the boundaries of a moving, molten layer, with effective internal convection and rapid transport of the excess heat from the upper boundary to the lower one.

A new technique based on the Stefan equation is introduced for calculation of the absorption and emission of heat that results from the effect of the latent heat of fusion of phase transitions occurring at two moving boundaries of a melt.

From the analysis presented in this paper, the following preliminary conclusions are made:

1. The introduction of thermal conductivity, decreasing toward the surface, increases the thermal insulation effect of the upper cover of the Moon and facilitates retention of the melt in the interior of the Moon for a period of 1.3 b.y., rather than 300 m.y. as for a uniform thermal conductivity of 0.007 cal/cm • s • °C.
2. A uniform distribution of uranium with a concentration of 60 ppm does not reflect the observed values of the heat flux because γ-spectrometry data indicate a sharp concentration of radioactive elements in the crust and their enrichment in the lunar highlands.
3. A distorting effect of the mare basin mascons on the observed heat fluxes is not excluded due to the different nature of these basins whose substance is more heat conducting and contains increased percentages of iron and titanium. The greatest distortions are expected near the edge of such basins where the heat-flux measurements were made. It is presently difficult to accurately predict the magnitude of the expected anomalies because of the shortage of data on the thermal conductivity coefficient of the matter making up the mascons.
4. The thermoelastic history of the Moon, analyzed with allowance for the expanding effect of the molten layer below the lithosphere, shows that the increase in the Moon's perimeter was sufficient for the formation of deep fractures through which lavas erupted and filled the mare basins. The eruption of lava was stimulated in the early history of the Moon by bombardment of the surface with meteorites.
5. During the life of the Moon, the emission of heat into space has gradually declined. At 1 AE after formation of the Moon, the heat flux reached 1.17×10^{-6} cal/cm^2 • s; after 3 AE, it decreased to 0.64×10^{-6} cal/cm^2 • s and almost stabilized. Since then subsequent decrease has not exceeded 10 to 15 percent.

Appendix 1: Analytical Solution

Heat calculations are carried out using a nonstationary thermal conductivity equation for a spherically symmetric planetary body (Moon, Mars, Mercury, asteroids, etc.), containing internal heat sources

$$C_p\rho \frac{\partial T}{\partial t} = \frac{1}{r^2}\frac{\partial}{\partial r}\left[r^2(\lambda_{cp} + \lambda_r)\frac{\partial T}{\partial r}\right] + H(r,t) \quad (1.1)$$

where C_p is the specific heat capacity, T is the temperature at point (r,t), ρ is the density, and $H(r,t)$ is a function of the heat source, which usually implies the long-lived, naturally radioactive isotopes U^{238}, U^{235}, Th^{232}, and K. The energy of gravitational differentiation given off in the process of evolution of the Earth, the latent heat of phase transitions, and other things can also be included in $H(r,t)$ (ref. 2).

The physically based boundary conditions are

$$\left.\begin{aligned} T(r = R,t) &= \text{Const} \\ \frac{\partial T}{\partial r}(r = 0,t) &= 0 \\ T(r,t = 0) &= T_0(r) \end{aligned}\right\} \quad (1.2)$$

For these conditions, the classical form of solution applicable to the radius of the Earth was obtained by Lowan (1936), Urey (ref. 7), and Kopal (ref. 48).

The expression for the temperature inside a sphere of radius R obtained by these researchers is presented in the form of an infinite series by trigonometric functions and, as Van Orstrand showed (ref. 49), the series converges very slowly. The use of Green's function, with application of the method of sequential reflections, gives considerably

more rapid convergence of the series. It also represents the temperature inside the sphere and the thermal flux on the surface in the form of a formula, permitting a clear physical interpretation. Construction of a solution for temperature is carried out in the following manner. The substitution of variables is

$$u = r \times T(r,t) \tag{1.3}$$

The boundary conditions will then be

$$u(z,0) = 0;\ u(R,t) = 0;\ u\ (0,t) = 0 \tag{1.4}$$

The expression for $u\ (r,t)$ is expressed through Green's function G:

$$u(r,t) = \int_0^t \int_0^R G(r,t,r',\tau)\ \frac{H(\tau)r'}{c\rho}\ dr'd\tau \tag{1.5}$$

where $G(r,t,r',\tau)$ is Green's function for the segment $[0,R]$

$$G(r,t,r'\tau) = \sum_{n=-\infty}^{\infty} [G_0(r,t,2nR+r',\zeta) - G_0(r,t,2nR-r'\tau)] \tag{1.6}$$

in which

$$G_0(r,t,r',\tau) = \frac{1}{2\sqrt{\pi\kappa(t-\tau)}}\ \exp\left[-\frac{(r-r')^2}{4\kappa(t-\tau)}\right] \tag{1.7}$$

Further, the variables are replaced,

$$r \pm 2nR \pm r' = y \tag{1.8}$$

and the expression for the temperature inside a spherical body takes the form

$$T(r,t) = \frac{1}{c\rho\sqrt{4\pi\kappa}}\ \frac{1}{r}\int_0^t \frac{H(\tau)}{\sqrt{(t-\tau)}} \left\{ \sum_{n=0}^{\infty} \int_{(2n-1)\ R-r}^{(2n+1)\ R-r} (r - 2nR + y)\exp\left[-\frac{y^2}{4\kappa(t-\tau)}\right] dy + \sum_{n=1}^{\infty} \int_{(2n+1)\ R-r}^{(2n+1)\ R+r} (r + 2nR - y)\exp\left[-\frac{y^2}{4\kappa(t-\tau)}\right] dy \right\} d\tau \tag{1.9}$$

After transformation of the sums and integrals, we have

$$T(r,t) = \frac{1}{c\rho}\int_0^t \mathrm{H}(\tau)\,dr - \frac{1}{c\rho}\ \frac{R}{r}\int_0^t H(\tau) \left[\sum_{n=0}^{-\infty} erfc\ \frac{(2n+1)R-r}{4\kappa(t-\tau)} - erfc\ \frac{(2n+1)R+r}{4\kappa(t-\tau)}\right] d\tau$$

The first term defines the temperature in the center; the second the magnitude of the outflow of the heat to the surface. Analysis of the convergence permits determination of the number of terms of the series $n \geq m$, starting with which, all subsequent terms of the series, with $m \geq 3\sqrt{Kt/R}$, can be discarded.

With thermal diffusivity of the rock on the order of $K = 0.01$ cm²/s, it holds true for the terrestrial planets and for intervals of time less than 5×10^9 yr that it is sufficient to take only one term of the series with $n = 0$, if the radius of the body is greater than $R = 1700$ km.

The temperature in the center of the planet or asteroid of any radius and at any moment of time is given by the expression

$$\mathrm{T}(r = o,t) = \lim_{r\to 0} T(r,t) = \frac{1}{c\rho}\int_0^t H(\tau)\,d\tau - \frac{R}{c\rho}\ \frac{1}{\sqrt{\pi}}\int_0^t \frac{H(\tau)}{\sqrt{K(t-r)}} \sum_{n=0}^{\infty} \exp\left[-\frac{(2n+1)^2\ R^2}{4K(t-\tau)}\right] d\tau$$

where

$$H(\tau) = \Sigma\, H_0^i\ \exp(-\lambda_i(t-\tau_0))$$

Appendix 2: Numerical Solution Without Consideration of Melting

The schemes commonly used previously had the shortcoming that, with small steps along the radius, too much machine time was required. Therefore, for example, MacDonald (ref. 8) had to limit the radius steps h to the order of 50 km; Toksöz and Solomon (ref. 23) and Mayeva (ref. 50) to a value $h = 20$ km; and Ornatskaya (ref. 13) to about 5 km. In this case, the fine structure of the lunar crust and the unique nature of the low coefficients of thermal conductivity of the outer crust of the Moon actually drop out of the analysis. Calculations of the surface heat flux at such h is extremely inaccurate. In this case, the effect of the irregular structure of the crust of the Moon is ignored. Limitations on stability are weakened by the use of implicit finite difference schemes. The error is

small for great depths, but it increases near the surface. In order to obtain a denser location of points near the surface, one can substitute variables

$$r = 1-x^2 \qquad (2.1)$$

Then the thermal conductivity equation will be approximated by the scheme described for equal new variable steps. The calculation involves use of the standard trial-run method, a convenient method for solution of the resulting system of linear equations "linked" to each other. The finite difference analog of the thermal conductivity equation, with irregular distribution of heat sources $H(r,t)$ and variable physical parameters ρ,λ,C_p at each point of the calculation network, has the form

$$T_i^{j+1} = \frac{1}{c(r_i)\rho(r_i)} \left\{ c(r_i)\rho(r_i) - \frac{\tau}{h^2 r_i} \left[r_{i+1}\lambda \left(\frac{T_{i+1}^j + T_i^j}{2}; \frac{r_{i+1}+r_i}{2} \right) + r_{i+1}\lambda \left(\frac{T_i^j + T_{i-1}^j}{2}; \frac{r_i + r_{i+1}}{2} \right) \right] T_i^j + \frac{\tau}{h^2 r_i} \left[r_{i+1}\lambda \left(\frac{T_{i+1}^j + T_i^j}{2}; \frac{r_{i+1}+r_i}{2} \right) T_{i+1}^j + r_{i-1}\lambda \left(\frac{T_i + T_{i-1}}{2}; \frac{r_i + r_{i-1}}{2} \right) T_{i-1}^j \right] + \tau H(r_i, t_j) \right\} \qquad (2.2)$$

Appendix 3: Consideration of the Latest Heat of Fusion.

The difference analog of the thermal conductivity equation, containing a change in heat content due to absorption or emission of the latent heat of fusion at the phase transition boundaries, has the form in dimensionsless variables

$$H'(Rr_i'; u_i^{j+1} \quad \frac{u_i^{j+1} - u_i^j}{2} = \frac{\kappa}{r_i^{j2}} \frac{1}{h} \left[\left(r'_i + \frac{h_{i+1}}{2} \right)^2 \lambda \left(\frac{u_{i+1}^{j+1} + u_i^{j+1}}{2}, R(r'_i + \frac{h_{i+1}}{2}) \right) \right] \frac{u_{i+1}^{j+1} - u_i^{j+1}}{} - \left[\left(r'_i - \frac{h_i}{2} \right)^2 \lambda \left(\frac{u_i^{j+1} + u_{i-1}^{j+1}}{2}, R(r_i - \frac{h_i}{2}) \right) \right] \frac{u_i^{j+1} - u_{i-1}^{j+1}}{h_i} \right]$$

$$+ H(Rr'_i, Lt_i^{j+1})L$$

where $t' = t/L$, $r' = r/R$

$$h_i = r'_i - r'_{i-1}$$

$$h_i = \frac{h_i + h_{i+1}}{2}$$

$$\Sigma h_i = 1, \ \kappa = L/R^2$$

References

1. TIKHONOVA, T. V., AND V. S. TROITSKY, Determination of the Heat Flux From the Interior of the Moon with the Heterogeneous Structure of Its Surface Layer. *Fizika Luny i Planet*, 1972, pp. 78–182.
2. LYUBIMOVA, YE. A., *Thermals of the Earth and Moon*, 1968.
3. RUSKOL, YE. L., Model of Accretion of the Moon Compatible with Data on the Composition and Age of Lunar Rock. *The Moon*, Vol. 6, 1973, pp.176–189.
4. KAULA, W. M., *Mechanical Processes Affecting Differentiation of Proto-Lunar Material.* This collection.
5. SOLOMON, S. C. AND M. N. TOKSÖZ, Internal Constitution and Evolution of the Moon. *Phys. Earth Planet. Interiors*, Vol. 7, 1973, pp. 15–38.
6. TOKSÖZ, M. N. AND D. H. Johnston, The Evolution of the Moon and the Terrestrial Planets. *Soviet-American Conference on the Cosmochemistry of the Moon and the Planets*, Moscow, June 4–8, 1974. This collection.
7. ORNATSKAYA, O. I., YA. I. AL'BER, AND I. L. RYAZANTSEVA, *Calculations of the Thermal History of the Moon with Various Concentrations of Radioactive Elements, Considering Differentiation of Matter in Melting.* This collection.
8. MACDONALD, G. J. F., Calculations on the Thermal History of the Earth. *J. Geophys. Res.*, Vol. 64, 1959, pp. 1967–2000.
9. MACDONALD, G. J. F., *Space Sci. Rev.* Vol. 2, 1963, p. 473.
10. UREY, H. C., Origin and History of the Moon. *Physics and Astronomy of the Moon*, 1962, p. 481.
11. LEVIN, B. YU., Thermal History of the Moon. *The Moon*, 1962, p. 157.
12. MAYEVA, S. V., Some Calculations of the Thermal History of Mars and the Moon. *Izv. Komiza Po Fizike Planet*, No. 5, 1965, pp. 49–70.
13. LYUBIMOVA, YE. A., Theory of the Thermal State of the Earth's Mantle. *The Earth's Mantle*, No. 4, 1967.
14. TROITSKIY, V. S., *Izv. VUZ Radiofizika*, Vol. 10, No. 8, 1967.

15. TINHONOVA, T. V., AND V. S. TROITSKY, Determination of the Heat Flux From the Interior of the Moon with the Irregular Structure of Its Surface Layer. *Fizika Luny i Planet*, 1972, pp. 178–183.
16. LANGSETH, M. G., S. J. KEIHM, AND J. L. CHUTE, JR., Direct Measurements of Heat Flow From the Moon. *Lunar Sci.*, 1973, pp. 445–456.
17. LANGSETH, M. G., S. J. KEIHM, AND J. L. CHUTE, JR., Heat Flow Experiment Apollo 17. *Preliminary Sci. Report, NASA*, 9–1, 9–24, 1973.
18. LATHAM, G., J. DORMAN, F. DUENNEBIER, M. EWING, D. LAMMLEIN, AND Y. NAKAMURA, Moonquakes, Meteoroids and the State of the Lunar Interior. *Lunar Sci. IV*, 1973, pp. 457–459.
19. ANDERSON, D. L., AND T. C. HANKS, The Moon. *Science*, Vol. 178, 1972, p. 1245.
20. ARKANI HAMED, J., Viscosity of the Moon. 1: After Mare Formation. *The Moon*, Vol. 6, 1973, pp. 100–111.
21. WOOD, J. A., Thermal History and Early Magmatism in the Moon. *Icarus*, Vol. 16, 1972, pp. 229–240.
22. VINOGRADOV, A. P., *Differentiation of Lunar Material.* This collection.
23. TOKSÖZ, N. M. AND S. C. SOLOMON, Thermal Evolution of the Moon. *The Moon*, Vol. 7, 1973, pp. 251–278.
24. LYUBIMOVA, YE. A., The Role of Radioactive Decay in the Thermal Regime of the Earth. *Izv Akad nauk SSSR Geofiz, Serial 2*, 1952, pp. 3–17.
25. LYUBIMOVA, YE. A., "Thermal History of the Earth with Consideration of the Variable Thermal Conductivity of Its Mantle." *Geophys. J. Roy. Astron. Soc.*, Vol. I, No. 2, 1958.
26. RINGWOOD, A. E., AND E. ESSENE, Petrogenesis of Lunar Basalts and the Internal Constitution of the Moon. *Science*, Vol. 167, 1970, pp. 607–610.
27. MIZUTANI, H., T. MATSUI, AND H. TAKEUCHI, Accretion Process of the Moon. *The Moon*, No. 4, 1972, pp. 476–489.
28. UREY, H. C., AND G. J. F. MACDONALD, Origin and History of the Moon. *Physics and Astronomy of the Moon*, No. 4, 1971, pp. 213–289.
29. KAULA, W. M., Interpretation of the Lunar Gravity Field. *Phys. Earth Planet. Interiors*, Vol. 4, 1971, pp. 185–192.
30. RINGWOOD, A. E., Evolution of the Solar System. *Geochimica et Cosmochimica Acta*, 1966.
31. HANKS, T. C., AND D. L. ANDERSON, Origin, Evolution and Present Thermal State of the Moon. *Phys. Earth Planet. Interiors*, Vol. 5, 1972, pp. 409–425.
32. HAYS, T. F., AND D. WALKER, *Lunar Igneous Rocks and the Nature of the Lunar Interior.* This Collection.
33. ANDERSON, D. L., The Composition and Origin of the Moon. *Earth Planet. Sci. Letters*, Vol. 18, 1973, pp. 301–316.
34. WOOD, J. A., J. DICKEY, V. B. MARVIN, AND B. N. POWELL, Lunar Anorthosites. *Science*, Vol. 167, 1970, p. 602.
35. TAYLOR, S. R., Chemical Evidence for Lunar Melting and Differentiation. *Nature*, Vol. 245, 1973, pp. 203–205.
36. LANGSETH, M. G. AND S. J. KEIHM, In Situ Measurements of Lunar Heat Flow. *Soviet-American Conference on the Cosmochemistry of the Moon and the Planets*, Moscow, June 4–8, 1974. This collection.
37. ANDERSON, D. L., The Interior of the Moon. *Phys. Today*, Vol. 4, 1974, p. 49.
38. TRIFONOV, V. G., AND P. V. FLORENSKIY, Discrete Dimensions of Round Mare and Thalassoids of the Moon. *Phys. Today*, Vol. 4, pp. 191–195.
39. WOOD, J. A., *Science*, Fourth Lunar Science Conference, Vol. 181, No. 4100, 1973, pp. 615–622.
40. SHURERT, G., D. L. TURCOTT, AND E. R. OXRURGH, Stability of Planetary Interiors. *Geophys. J. Rev. Astron. Soc.* Vol. 18, 1969, p. 441.
41. SURKOV, YU. A., AND G. A. FEDOSEYEV, *Radioactivity of the Moon, Planets and Meteorites.* This collection.
42. LANGSETH, M. G., JR., S. P. CLARK, JR., G. L. CHUTE, JR., S. J. KEIHM, AND A. E. WECHSLER, The Apollo 15 Lunar Heat Flow Measurement. *The Moon*, Vol. 4, 1972, pp. 390–410.
43. CLARK, S. P., JR., Handbook of Physical Constants. *Geol. Soc. Am. Memoir*, 1966, p. 97.
44. TROITSKIY, V. S., O. B. SHCHUKO, V. N. GOL'DBERG, AND L. V. DROBOVA, Determination of the Density of the Outer Crust of the Moon by Specified Temperatures of the Surface During Eclipses and the Lunar Night. *Izv. VUZ Radiofizika*, Vol. 10, No. 8, 1972, pp. 48–52.
45. SCHMITT, H. H., AND E. A. CERNAN, A Geological Investigation of the Taurus-Littrow Valley. *Apollo 17 Prelim. Sci. Report, NASA*, 5–1;–5–21, 1973.
46. TOKSÖZ, M. N., S. C., SOLOMAN, J. W. MINEVE, AND D. H. JOHNSTON, Thermal Evolution of the Moon. *The Moon*, Vol. 4, 1972, pp. 190–213.
47. KOVACH, R. L., J. S. WATKINS, AND P. TALWANI, Lunar Seismic Profiling Experiment Apollo 17. *Prelim. Sci. Report, NASA*, 10–1;–10–12, 1973.
48. KOPAL, Z., *The Moon*, 1962.
49. VAN ORSTRAND, C. E., Geothermal Methods of Estimating the Age of the Earth. *Geophys.*, Vol. 5, 1940.
50. MAYEVA, S. V., The Thermal History of the Terrestrial Planets. *Astrophys. Letter*, Vol. 4, 1968, pp. 11–16.